Volume 12 | Number 21 | 7 June 2014 | Pages 3313–3514

Organic & Biomolecular Chemistry

www.rsc.org/obc

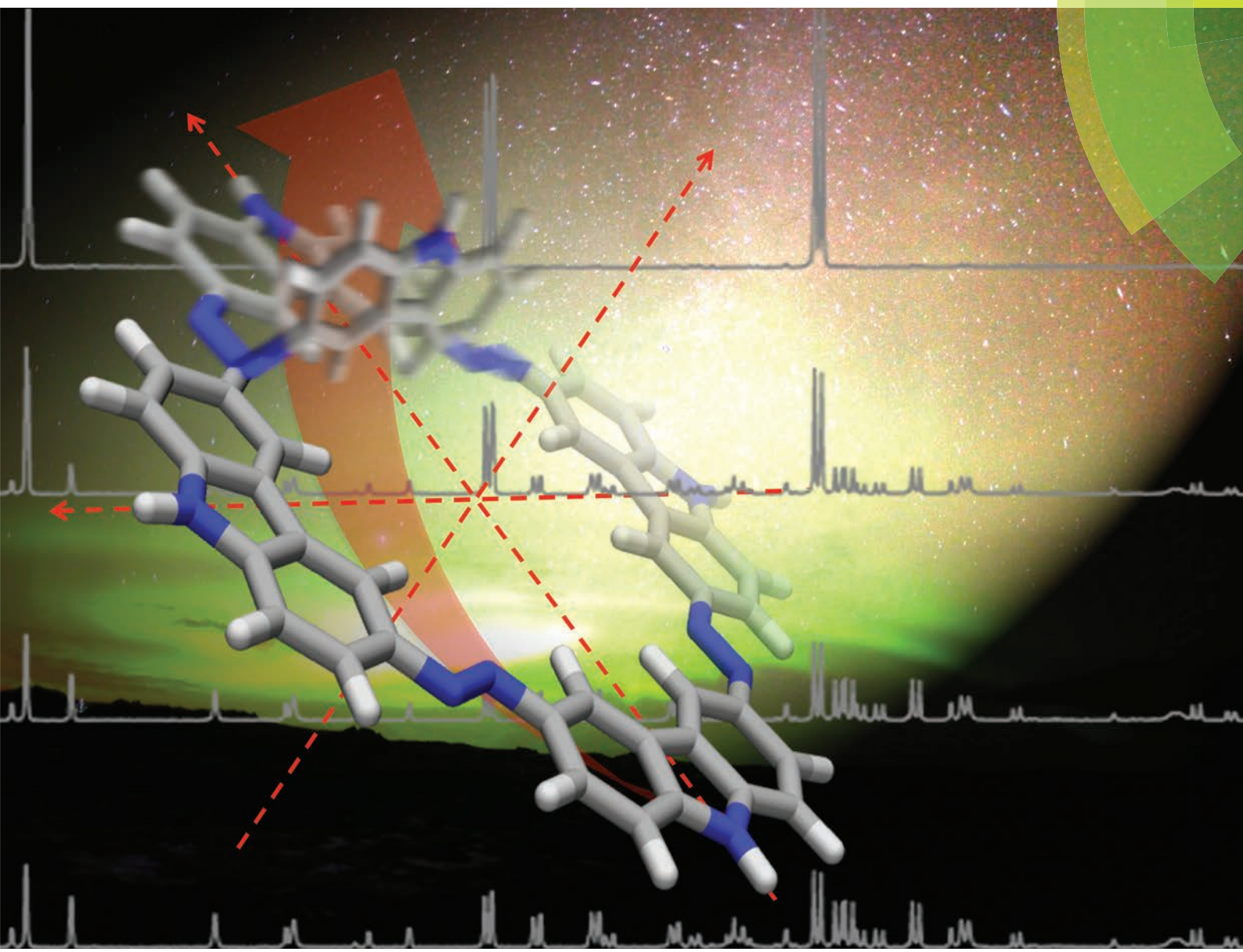

ISSN 1477-0520

ROYAL SOCIETY OF CHEMISTRY

PAPER
Hermann A. Wegner *et al.*
Symmetry as a new element to control molecular switches

Organic & Biomolecular Chemistry

PAPER

View Article Online
View Journal | View Issue

Cite this: *Org. Biomol. Chem.*, 2014, **12**, 3371

Symmetry as a new element to control molecular switches†

Luca Schweighauser,[a] Daniel Häussinger,[b] Markus Neuburger[b] and Hermann A. Wegner*[a]

Received 29th January 2014,
Accepted 27th February 2014

DOI: 10.1039/c4ob00230j

www.rsc.org/obc

The isomerization properties of an azocarbazole macrocycle in solution were investigated utilizing NMR spectroscopy with *in situ* irradiation in combination with DFT calculations. It was demonstrated that the position of azo units in a rigid macrocyclic system influences the photoisomerization pathway even if the initial all-*E* isomer is highly symmetric. Furthermore, the effect of ring strain on lowering the rates of thermal isomerization was demonstrated and a mechanism *via* an inversion–rotation proposed. The herein presented results and methods give new insights into the general nature of the azobenzene unit. In particular we illustrate the effect of symmetry changes due to macrocyclic arrangement on the photochemical and thermal isomerization properties, which will stimulate future development towards multinary molecular switches.

Introduction

Controlling the structure at the molecular level in a defined and reversible way promises tremendous opportunities in the area of molecular materials, for example as data storage devices,[1–3] sensors[4] or molecular machines,[5,6] but also for life science applications.[7–11] Especially light induced molecular switches have gained huge attention during the last decade due to their fast, selective and reversible switching properties.[12–14] Well-known scaffolds are for example diarylethenes,[15–17] spiropyrans[18,19] or azobenzenes.[20–29] The latter have emerged from classical dyes and have become powerful molecular switches due to their ability to alter the geometry by photochemical or thermal isomerization.[30,31] In most cases this switch works without any degradation, which makes azo chemistry a high potential approach to introduce mechanical movement into molecular systems.[32–35] Two mechanisms for this geometrical change were usually discussed in the past: planar inversion or a rotation around the N–N double bond.[36–39] Inversion was described to be the preferred mode for strained systems. Recently, additional pathways such as concerted inversion or inversion-assisted rotation were reported.[40]

However, the light induced *Z* isomer of azobenzene can be rather unstable because it undergoes thermal back isomerization to the thermodynamically more stable *E* isomer. An effective approach is the incorporation of azobenzenes into macrocyclic scaffolds,[41] which can have a dramatic influence on the switching properties due to the stabilization of the *Z* isomers by ring strain. In general, shape-persistent macrocycles[42] were found to have a wide range of applications such as self-assembly on surfaces[43,44] or self-aggregation into supramolecular channels.[45,46] In addition, macrocyclization offers the possibility to assemble multiple azo units to access several different states in one molecule. The strain induced in the switching process should also allow the differentiation of these states. Such macrocyclic arrangements can be of high interest in the field of molecular computing opening a new chapter in azobenzene chemistry. The design of macrocyclic oligo-azobenzenes offers special challenges because additional parameters besides ring strain and the number of azo moieties influence the isomerization properties. Such factors are, for instance, the rigidity and substitution of linkers connecting the azo units, the symmetry of the macrocycle or the degree of conjugation (Scheme 1).

Various questions concerning the effect of ring strain, the interaction between different azo units and the isomerization pathways of macrocyclic systems are still not fully answered. Rigid macrocyclic oligo-azo compounds with more than three azo units were not precisely studied in the past. Examples of studies on macrocyclic systems with four azo units connected by alkyl linkers were reported *e.g.* by the group of Tamaoki.[47–50]

[a]*Institute of Organic Chemistry, Justus-Liebig University, Heinrich-Buff-Ring 58, 35392 Giessen, Germany. E-mail: hermann.a.wegner@org.chemie.uni-giessen.de; Fax: +49 641-9934349*

[b]*Department of Chemistry, University of Basel, St. Johanns-Ring 19, 4056 Basel, Switzerland*

† Electronic supplementary information (ESI) available: Spectral data, NMR set-up details, crystallographic data and computational data are provided. CCDC 966041. For ESI and crystallographic data in CIF or other electronic format see DOI: 10.1039/c4ob00230j

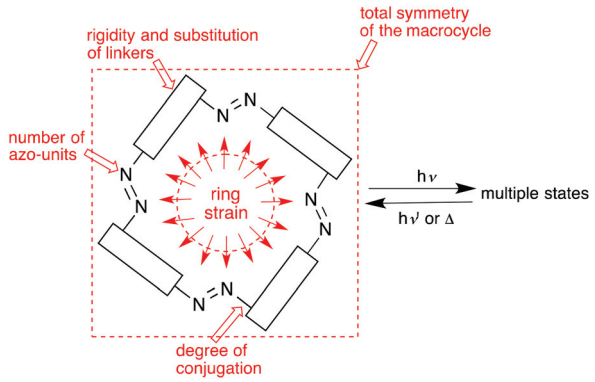

Scheme 1 Parameters for the design of macrocyclic azobenzenes influencing their isomerization properties to construct multinary molecular switches.

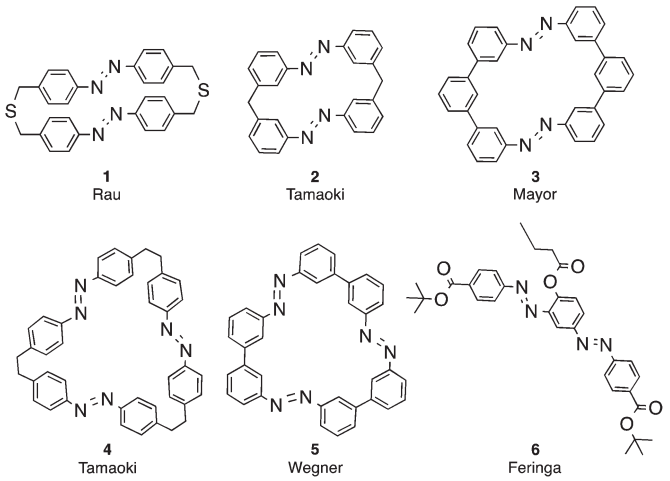

Fig. 1 Oligoazobenzenes containing two or three azo units by Rau, Mayor, Tamaoki, Feringa and our group. Nevertheless, none of the systems allowed the differentiation of identical substituted azo units only by changes of symmetry induced through the cyclic arrangement.

Rigid tetraazo systems are highly interesting, as they should allow a differentiation of azo units by symmetry, although the initial all-*E* isomer is highly symmetric. Due to the fact that after one azo unit is isomerized to the *Z* isomer, the second switching process can take place either on the opposite entity or just nearby (Scheme 2). Thus, two different isomers are formed after the second isomerization displaying different symmetry properties. A preference is, however, expected. Hence, complex systems with four incorporated azo units should allow the construction of multinary switches selecting certain states simply by exploiting symmetry considerations and their consequences.

Systems with multiple azo units pose demanding analytical challenges due to the formation of complicated mixtures after irradiation. These mixtures contain numerous isomers with various symmetries. Therefore, general and simple to apply methods are necessary to cope with these issues in order to support the development towards multinary molecular switches for highly sophisticated applications.

Among others, the groups of Rau,[51] Tamaoki,[52–54] Mayor[55] and our group[56] have shown that in macrocycles containing two or three azo units (Fig. 1) the rate of thermal isomerization was dependent on the ring strain of the specific isomer. On the other hand, for instance the group of Feringa[57] demonstrated isolated and, therefore, independent thermal isomerization of different azo units in case of linear multi-azo compounds.

On this account we designed a macrocycle composed of four azo and four carbazole units (Fig. 2). The carbazole moieties were substituted with alkyl chains for better solubility. Hecht and co-workers investigated the influence of electronic conjugation on the switching behaviour of two linear *para*-benzene-connected azo units.[58] They described a large improvement of the photochemical isomerization properties by decreasing the electronic conjugation. Electronic decoupling led to a separation of the absorption spectra of the involved states and to a large increase of the *Z*-content in the mixture after irradiation with a specific wavelength. This discovery was taken into consideration for the design of tetraazocarbazole macrocycle **7**. Our group has already reported its synthesis and reversible protonation properties in chlorinated solvents under UV-light irradiation earlier.[59]

The structure of macrocycle **7** offered the opportunity to analyse a demanding multinary switch, the interaction of different identically substituted azo units, the effect of ring strain and the thermal isomerization mechanism in strained

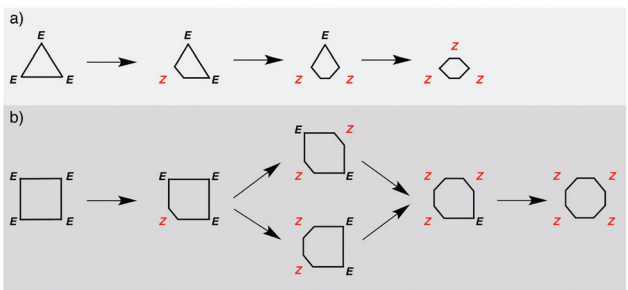

Scheme 2 (a) Symmetrically substituted azo trimer: only one isomer is possible after two units are isomerized; (b) symmetrically substituted azo tetramer: two isomers are possible after the second isomerization.

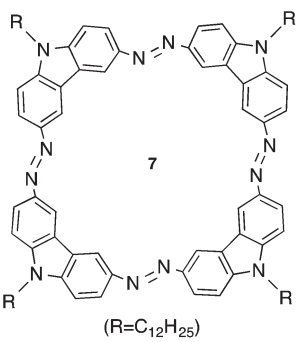

Fig. 2 Structure of macrocycle **7**.

systems. Insights into these effects will give a better understanding of the still debated mechanism of isomerization of azobenzenes. Herein, we present an extensive study on the solid-state structure, the isomerization properties and the reaction pathway by using X-ray crystallography, NMR spectroscopy and computational methods.

Results and discussion

X-Ray crystallography

Crystallographic investigations give important information about macrocyclic systems in the solid state, for example, about the influence of long alkyl chains on solid-state packing. Nevertheless, only a few reports on X-ray data of such molecules exist in the literature due to large difficulties in crystallization and disordering. In addition, volatile solvents often crystallize into the cavities formed by large macrocycles leading to decomposition of crystals before analysis.[60] The all-*E* isomer of macrocycle **7** was crystallized by slow evaporation of the solvent from a chloroform/benzene solution. The product crystallized in the monoclinic crystal system in space group $P2_1/n$. In the crystal packing the alkyl chains were organized in an alternating way and build a layer between the macrocycles resulting in a "zigzag" pattern (Fig. 3). Moore *et al.* reported a similar effect for carbazole–ethynylene macrocycles.[61] The macrocycle deviates slightly from planarity. The smallest diameter of the ring measured between two azo units was 10.8 Å and 16.6 Å between the carbazole nitrogen atoms. The distance between the alkyl chains and the macrocyle was 3.6 Å, hinting at a significant interaction of those. Due to the alternating alkyl chains positioned above and below each macrocycle the smallest distance between two rings was 7.2 Å. From C9 onwards the alkyl chains were slightly disordered and curved. Solvent molecules did not crystallize inside the macrocycle cavities; the curved alkyl chains filled the space instead. Benzene molecules crystallized in the packing outside the macrocycles.

NMR spectroscopy

Solutions of macrocycle **7** in $CDCl_3$ showed a significant high field shift of the aromatic signals in the ^{1}H-NMR spectrum with increasing concentration of the sample (Fig. 4), which can be explained by aggregation *via* stacking. This stacking behaviour was evidence for a high organization of macrocycle **7** not only in the solid state but also in solution. It has been shown before that oligo-azobenzene macrocycles are able to change the strength of aggregation reversibly by light.[63,64]

UV/VIS spectroscopy

The absorption spectrum of the initial all-*E* isomer of macrocycle **7** showed a broad absorbance with a maximum at 422 nm. As we have already reported earlier, irradiation with UV-light at 302 nm in chlorinated solvents led to a reversible protonation and was accompanied by a strong colour change.[59] These protonation properties made macrocycle **7**

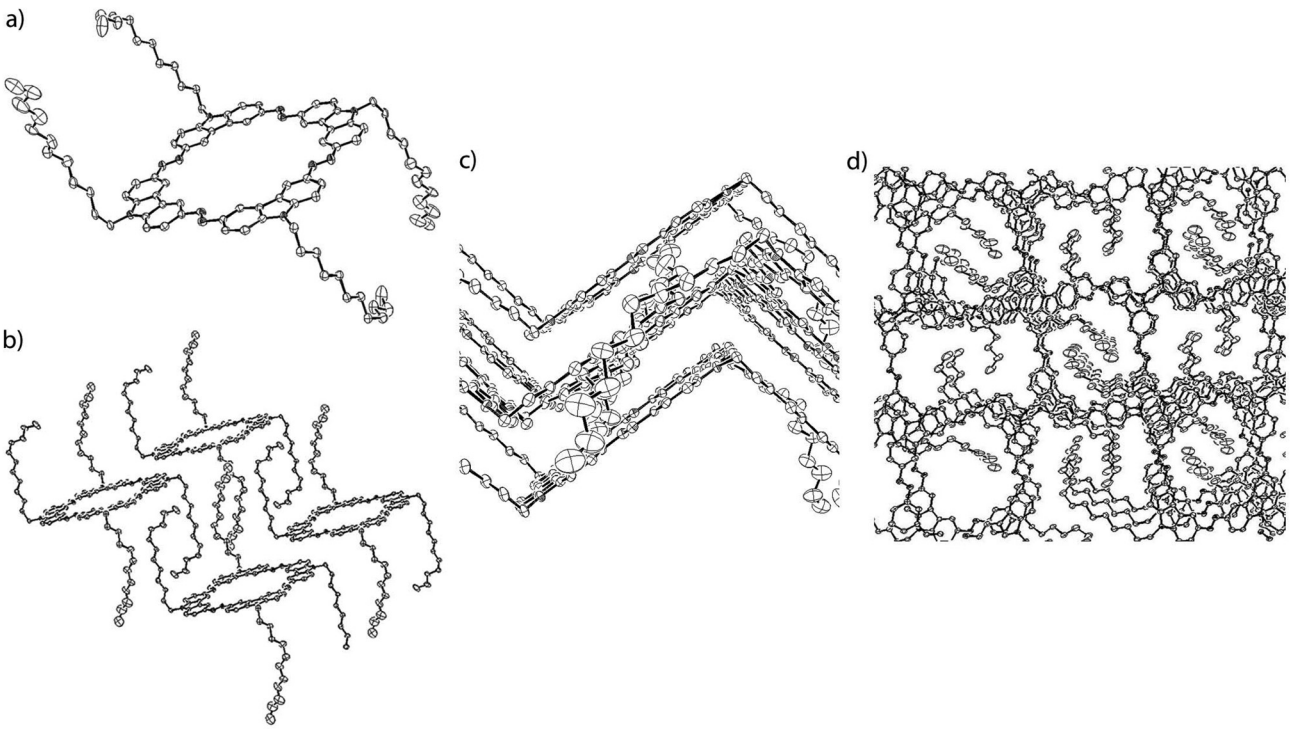

Fig. 3 (a) X-ray structure of the all-*E* isomer of macrocycle **7**; (b) representation of the alternating alkyl chains; (c) layers of alkyl chains are sandwiched between the macrocycles; (d) the alkyl chains fill the space inside the macrocycle cavities (ORTEP, ellipsoids drawn at the 50% probability level; hydrogen atoms and solvent have been omitted for clarity).

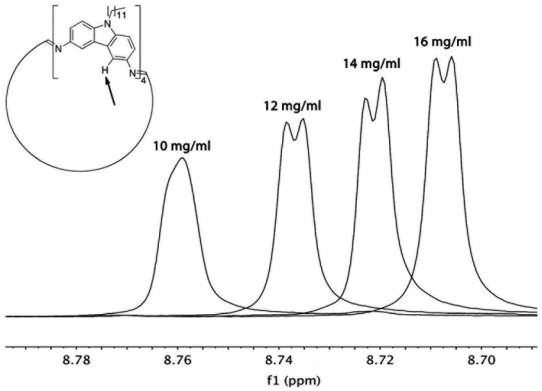

Fig. 4 Aggregation in solution was represented by a concentration dependent shift in the ^{1}H-NMR spectrum (in $CDCl_3$, 25 °C). The displayed NMR signal appears as a doublet due to $^{4}J_{HH}$-coupling.[62]

suitable for application as a molecular logic gate but hindered almost the entire isomerization process. Therefore, irradiation with light at the absorption maximum to analyse the switching properties was conducted in THF.

Upon irradiation with light at 424 nm the absorption maximum decreased but the development of a new absorption band was not monitored (Fig. 5). This observation was rationalized by the explanation that the absorption maxima of the generated isomers are very close to the maximum of the all-*E* isomer. Thus, all isomers were irradiated at the same time leading to a photostationary state consisting of a mixture of isomers.

NMR isomerization studies

NMR spectroscopy was found to be the preferred experimental method to get a deep insight into the isomerization of complex multi-azo compounds as it gives precise structural information in solution. Nevertheless, access to the sample and, therefore, the possibilities for performing manipulations such as irradiation during measurements is limited due to the technical set-up of an NMR machine. In addition, time-consuming NMR experiments make analysis of labile states and compounds challenging.

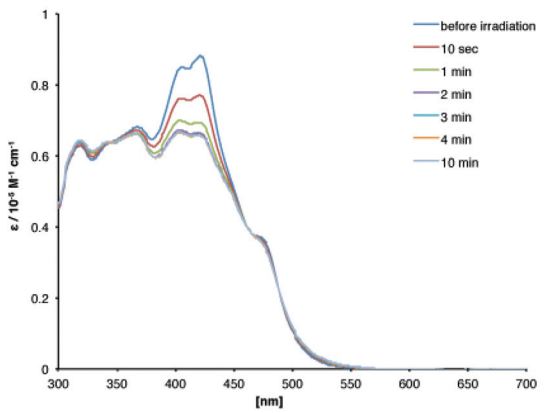

Fig. 5 Absorption spectrum of macrocycle **7** in THF when irradiated with light at 424 nm over different time periods.

The initial thermodynamic stable all-*E* isomer of macrocycle **7** showed the expected highly symmetric ^{1}H-NMR spectrum with three signals in the aromatic region. Upon irradiation with light at 424 nm a complex mixture of different isomers with various symmetries was formed, making assignment by simple one-dimensional ^{1}H-NMR spectroscopy impossible. For a complete assignment of all proton signals two-dimensional NMR experiments in the thermally unstable photostationary state as well as knowledge of the isomeric composition at any time of the process were necessary. For that reason a method had to be developed to keep macrocycle **7** in the photostationary state for several hours within the NMR spectrometer. Analysis *via* isolation or separation by *e.g.* HPLC was deliberately not applied, as the larger time frame required might distort the measurement.

A monochromator designed for fluorescence microscopy fitted with an optical fibre was attached to the spectrometer. The end of the optical fibre was adjusted to be just in contact with the sample solution in order to minimize photon losses, but without deteriorating the homogeneity of the magnetic field. This experimental setting allowed to record NMR spectra while the sample was irradiated without the need for special laser equipment (Fig. 6a).[65] The drawback of using this light source was the relatively weak irradiation intensity. Therefore, the concentration of the sample was reduced to 125 μM to achieve sufficiently high isomerization. This modification also reduced the formation of aggregates in solution drastically.

Under these conditions two-dimensional ROESY, COSY and long-range COSY (optimized to a delay of 100 ms for aromatic $^{4}J_{HH}$-coupling) NMR experiments were conducted enabling to assign which signals relate to which carbazole unit. This way it could also be determined which carbazole units were symmetric and which non-symmetric. However, it did not allow assigning which carbazole units are connected. This information was determined by comparing the rates of appearance of the different signals in ^{1}H-NMR experiments upon irradiation as well as the rates of thermal back isomerization to the all-*E* isomer (Fig. 7). Combination of all this information allowed assigning the isolated carbazole spin systems to the different isomers. Determining the symmetries of all six possible isomers with molecular models finally enabled the characterization of the observed isomers (Fig. 6b).

The 125 μM solution of macrocycle **7** in THF reached the photostationary state (pss) after 73 min when irradiated with light at 424 nm. Five of six possible isomers could be identified. Only the all-*Z* isomer was not observed or insufficient quantities were in the sample to be detected. The mixture at the photostationary state contained mainly the (*E*,*E*,*E*,*Z*) (49%), the initial all-*E* (21%) and the (*E*,*E*,*Z*,*Z*) (19%) isomers (Fig. 8). The (*E*,*Z*,*E*,*Z*) (7.2%) and the (*E*,*Z*,*Z*,*Z*) (4.0%) were detected in minor quantities. Increasing the temperature to 50 °C resulted in a much higher ratio of the all-*E* isomer in the photostationary state but in less quantities of the (*E*,*E*,*E*,*Z*) (32%), the

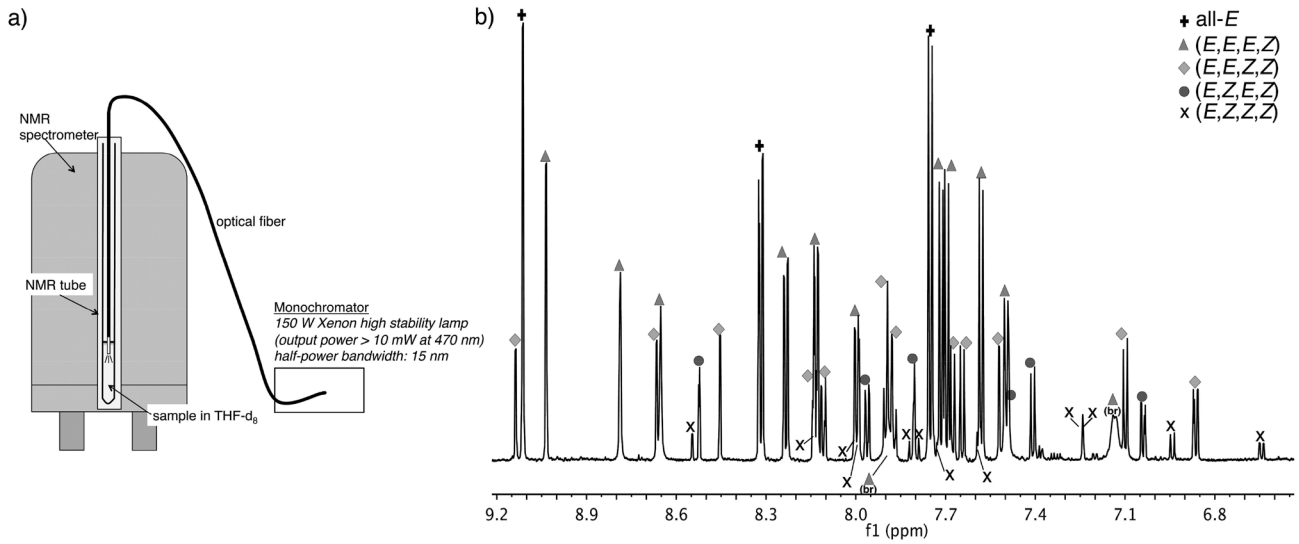

Fig. 6 (a) Experimental set-up to perform NMR experiments while the sample was irradiated; (b) aromatic region of the ^{1}H-NMR spectrum and assignment of the aromatic signals of macrocycle **7** after irradiation with light at 424 nm in THF-d_8.

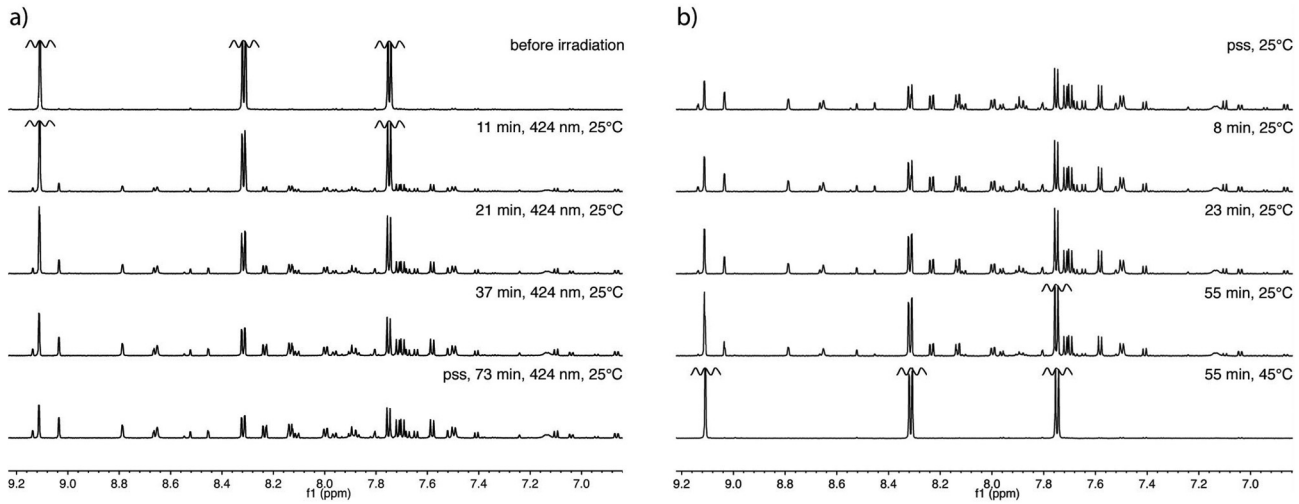

Fig. 7 (a) Formation of the different isomers upon irradiation with light at 424 nm in THF-d_8; (b) thermal back reaction to the thermodynamic stable all-*E* isomer under exclusion of light in THF-d_8.

(*E*,*E*,*Z*,*Z*) (4%) and the (*E*,*Z*,*Z*,*Z*) (1.7%) isomers. Remarkably, the ratio of the (*E*,*Z*,*E*,*Z*) (6.8%) has remained almost unchanged.

Various isomers formed upon irradiation with very different rates. The rate decreased in general with increasing the number of azo units, which were isomerized from *E* to *Z* (Fig. 9a). All four isomers reached the photostationary state at the same time with a continuously increasing ratio (Fig. 9b). There was no accumulation of one specific isomer observed and only the all-*E* isomer concentration decreased during the irradiation process. As the photochemical isomerization follows a step-by-step pathway, which means that the isomers develop one upon the other, this observation illustrated that all isomers absorbed within the irradiated wavelength promoting a photochemical isomerization not only from *E* to *Z* but also from *Z* to *E*.

Interestingly, there were only small amounts of the (*E*,*Z*,*E*,*Z*) isomer in the mixture after irradiation, which showed that (*E*,*E*,*Z*,*Z*) was favoured in the photostationary state. Tamaoki and co-workers observed also a preference of 2 : 1 for the (*E*,*E*,*Z*,*Z*) isomer.[49] However, in their case this ratio was constant under all investigated conditions. Therefore, the preferred formation of the (*E*,*E*,*Z*,*Z*) isomer was rationalized by statistical reasons as there are two possibilities to form the (*E*,*E*,*Z*,*Z*) isomer compared to only one for the (*E*,*Z*,*E*,*Z*) isomer. For compound **7** the ratio measured (1 : 2.64 at 25 °C) and the dramatic change by increasing temperature (1 : 0.59 at 55 °C) show clearly that the ratio of isomerization between the (*E*,*Z*,*E*,*Z*)

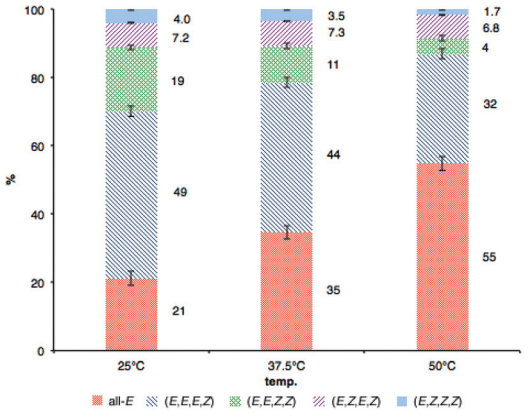

Fig. 8 Composition in the photostationary state at different temperatures.

and the (*E*,*E*,*Z*,*Z*) isomer is not only controlled by statistics. Although conjugation is limited in the ground state, due to the *meta*-connection of the parent azobenzene subunits, this behaviour can change in the excited state (Baird's rules). Hence, symmetry arguments, which play a major role in photochemical processes, should be observable. Kuhn showed already in 1949 that the absorption of symmetric compounds differs from asymmetric ones (in the example of polymethine dyes), which can be taken as a reference for the above formulated reasoning.[66]

In addition, according to the photochemical NMR experiments it could be assumed that the different rates of (*E*,*Z*,*E*,*Z*) and (*E*,*E*,*Z*,*Z*) formation under irradiation were based on thermal stability of the specific isomers. Nevertheless, the thermal isomerization study showed that this explanation was not accurate. Although both isomers have two azo units in *Z* configuration, it is proposed that the different macrocyclic symmetries were allowing a photochemical differentiation between the (*E*,*E*,*Z*,*Z*) and the (*E*,*Z*,*E*,*Z*) isomer. Therefore, varying isomerization rates presumably depend on different quantum yields as well as slight changes in the absorption maxima. This discovery indicates that symmetry differences induced by the macrocyclic arrangement also lead to differentiation of states.

Looking at the thermal isomerization back to the initial all-*E* isomer, the rates were not in relation to the number of azo units in *Z* configuration (Fig. 9c). The (*E*,*Z*,*E*,*Z*) isomer appeared to have the highest and the (*E*,*E*,*Z*,*Z*) the lowest thermal stability (Fig. 9d). This observation illustrated the strong influence of ring strain on thermal isomerization.

Calculations

In order to get a deeper insight into the thermal isomerization and the thermal stabilities of the different isomers, it was important to know the activation enthalpies and free energies of activation for the formation of each isomer. For that reason the complete thermal isomerization pathway was calculated by DFT-calculations.[67] With these insights calculations can be applied as a powerful tool for the design of new macrocyclic oligo-azobenzenes and potentially predicting their (thermal) isomerization behaviour. DFT-calculations were conducted for

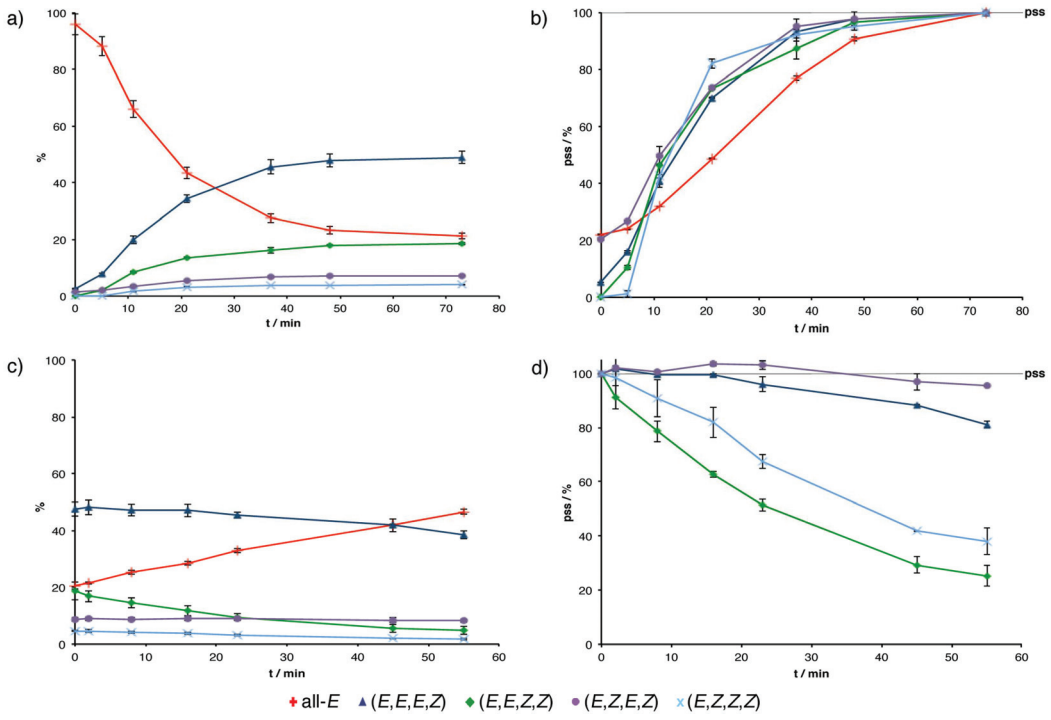

Fig. 9 (a) A solution of macrocycle **7** in THF-d_8 upon irradiation of light at 424 nm; (b) development of the photostationary state (pss) upon irradiation with light at 424 nm; (c) thermal isomerization back to the all-*E* isomer in THF-d_8 at 25 °C under exclusion of light; (d) relative decrease of the different *Z*-containing isomers after stopping irradiation.

the electronic ground state on the B3LYP level with a 6-311G(d, p) basis set. Hence, the calculations were accurate for the thermal isomerization pathway while the process induced by photoexcitation occurs on a different potential energy surface.

The determined transition states were close to the expected linear N–N–C conformation for strained systems indicating a thermal isomerization from *Z* to *E* *via* an inversion. However, the transition state deviates from linearity due to necessary rotation because of the macrocyclic structure.

The mechanism can be studied for example by looking at the isomerization from three dimensional (*E*,*E*,*E*,*Z*) to the planar all-*E* isomer. An exclusively inversion type mechanism would not allow rotation of the carbazole units into a planar structure. Therefore, a mixed mechanism with inversion and rotation is suggested for thermal isomerization (Fig. 10). The dihedral angle (C–N–N–C) and one of the C–N–N angles changed during the isomerization process, whereas the second C–N–N angle remained almost constant (Fig. 11).

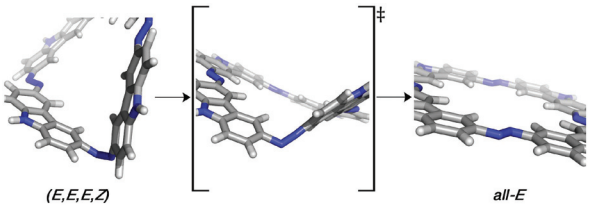

Fig. 10 Isomerization *via* an inversion–rotation mechanism.

The calculated kinetic parameters represent the effect of ring strain on the stabilization of *Z*-isomers (Table 1). The linear 9,9-methyl-3-azocarbazole was reported to have a rate constant of $k = 3.71 \times 10^{-5}$ s^{-1} and the linear 9,9-ethyl-3-azocarbazole $k = 4.97 \times 10^{-5}$ s^{-1}.[68] The calculated values for macrocycle **7** range from rather high $k = 7.45 \times 10^{-5}$ s^{-1} for the (*E*,*E*,*Z*,*Z*) to (*E*,*E*,*E*,*Z*) isomerization to very low $k = 3.77 \times 10^{-7}$ s^{-1} for the (*E*,*Z*,*E*,*Z*) to (*E*,*E*,*E*,*Z*) isomerization. Therefore, the rate of thermal isomerization is strongly dependent on the ring strain of the specific isomer. The activation entropy ($\Delta^{\ddagger}S$) is close to zero for all isomerization steps, which might be expected for a rigid macrocyclic ring system such as **7**. The calculation supports the study on thermal isomerization made by using NMR spectroscopy, which is also indicating that the (*E*,*Z*,*E*,*Z*) is relatively the most stable and the (*E*,*E*,*Z*,*Z*) the most unstable isomer in the system.

In general, the calculated kinetic parameters were in good agreement with the measured data, showing the effect of ring strain and providing information about the mechanism of thermal isomerization.

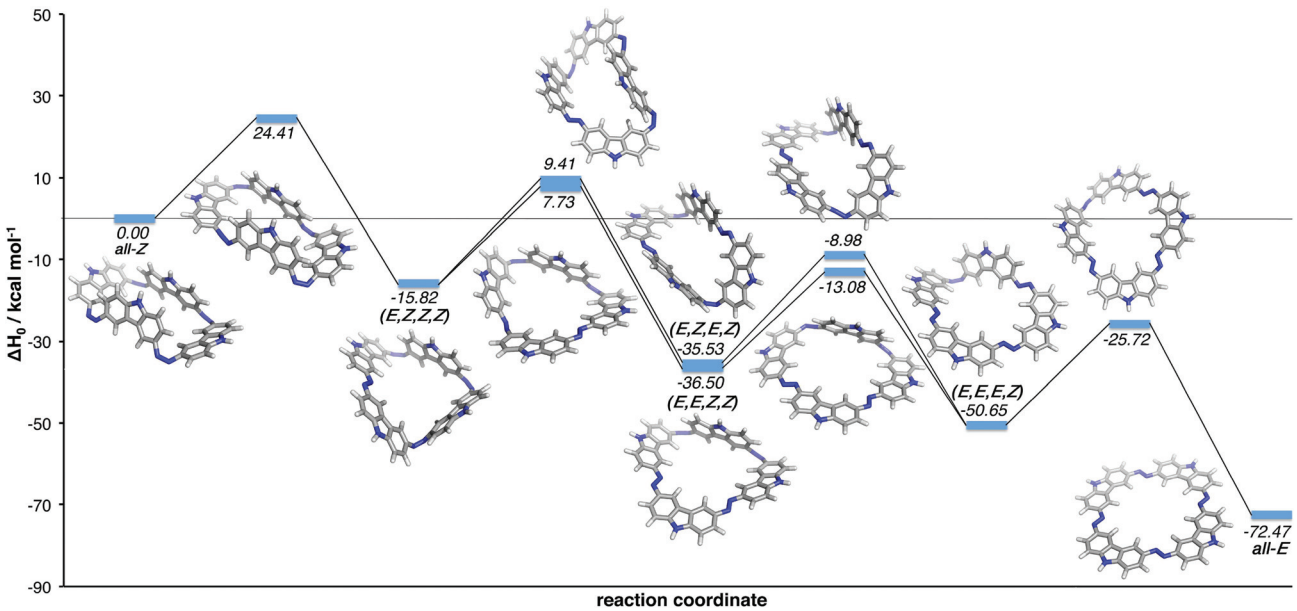

Fig. 11 Thermal reaction pathway from all-*Z* to all-*E*.

Table 1 Kinetic parameters of the thermal isomerization pathway

	$\Delta^{\ddagger}G°$/kcal mol^{-1}	$\Delta^{\ddagger}H°$/kcal mol^{-1}	$\Delta^{\ddagger}S$/cal K^{-1} mol^{-1}	k_{298K}/s^{-1}
All-*Z* → (*E*,*Z*,*Z*,*Z*)	24.14	24.52	1.29	1.25×10^{-5}
(*E*,*Z*,*Z*,*Z*) → (*E*,*E*,*Z*,*Z*)	23.57	23.55	−0.07	3.28×10^{-5}
(*E*,*Z*,*Z*,*Z*) → (*E*,*Z*,*E*,*Z*)	25.27	25.21	−0.18	1.88×10^{-6}
(*E*,*E*,*Z*,*Z*) → (*E*,*E*,*E*,*Z*)	23.08	23.47	1.29	7.45×10^{-5}
(*E*,*Z*,*E*,*Z*) → (*E*,*E*,*E*,*Z*)	26.22	26.59	1.26	3.77×10^{-7}
(*E*,*E*,*E*,*Z*) → all-*E*	24.47	24.99	1.75	7.22×10^{-6}

Conclusions

Herein, an extensive isomerization study on a fully characterized macrocycle containing four azo units is presented. The study combined data from UV/VIS absorption spectroscopy, NMR spectroscopy with *in situ* light irradiation and DFT calculations. The investigation illustrated the influence of macrocyclic symmetry and ring strain on the photochemical as well as the thermal isomerization pathways. A general experimental NMR method and a strategy for the analysis of isomer mixtures in the photostationary state were presented in order to investigate complex molecular photochemical switches. It could be demonstrated that the (*E*,*E*,*Z*,*Z*) isomer is preferred to the (*E*,*Z*,*E*,*Z*) isomer in the photostationary state and that simply the different position within the macrocyle allows this photochemical differentiation. Therefore, different states could be selected without the incorporation of specific substituents or irradiation with different wavelengths, but by the position of the azo units in the ring system influencing the overall symmetry of the molecule. The rate constants of the thermal isomerization steps of macrocycle **7** were in general smaller than those of comparable linear carbazole compounds. The highest free energy of activation was calculated and observed for the (*E*,*Z*,*E*,*Z*) isomer indicating a strong influence of ring strain. Furthermore, on the thermal isomerization pathway it was demonstrated that DFT-calculations lead to kinetic parameters that are comparable to experimental results. An inversion–rotation mechanism was proposed in order to explain the thermal switching properties of macrocycle **7**. Calculations are, therefore, an efficient tool in the design of new macrocyclic oligo-azobenzenes. The presented results and methods give important knowledge for the future design of azobenzene based molecular switches and allow investigations on highly complex systems supporting their development towards functional materials for sophisticated applications.

Acknowledgements

We thank Hubert Sperlich (Telegärtner Gerätebau GmbH, Klingenberg, Germany) as well as ScienTec (France) for their support in setting up the optical fibre installation.

Notes and references

1 J. E. Green, J. Wook Choi, A. Boukai, Y. Bunimovich, E. Johnston-Halperin, E. DeIonno, Y. Luo, B. A. Sheriff, K. Xu, Y. Shik Shin, H.-R. Tseng, J. F. Stoddart and J. R. Heath, *Nature*, 2007, **445**, 414–417.
2 E. Orgiu, N. Crivillers, M. Herder, L. Grubert, M. Pätzel, J. Frisch, E. Pavlica, D. T. Duong, G. Bratina, A. Salleo, N. Koch, S. Hecht and P. Samorì, *Nat. Chem.*, 2012, **4**, 675–679.
3 J. W. Brown, B. L. Henderson, M. D. Kiesz, A. C. Whalley, W. Morris, S. Grunder, H. Deng, H. Furukawa, J. I. Zink, J. F. Stoddart and O. M. Yaghi, *Chem. Sci.*, 2013, **4**, 2858–2864.
4 B. Champagne, A. Plaquet, J.-L. Pozzo, V. Rodriguez and F. Castet, *J. Am. Chem. Soc.*, 2012, **134**, 8101–8103.
5 E. R. Kay, D. A. Leigh and F. Zerbetto, *Angew. Chem., Int. Ed.*, 2007, **46**, 72–191.
6 B. Lewandowski, G. D. Bo, J. W. Ward, M. Papmeyer, S. Kuschel, M. J. Aldegunde, P. M. E. Gramlich, D. Heckmann, S. M. Goldup, D. M. D'Souza, A. E. Fernandes and D. A. Leigh, *Science*, 2013, **339**, 189–193.
7 S. Venkataramani, U. Jana, M. Dommaschk, F. D. Sonnichsen, F. Tuczek and R. Herges, *Science*, 2011, **331**, 445–448.
8 A. Mourot, M. A. Kienzler, M. R. Banghart, T. Fehrentz, F. M. E. Huber, M. Stein, R. H. Kramer and D. Trauner, *ACS Chem. Neurosci.*, 2011, **2**, 536–543.
9 D. Ray, J. T. Foy, R. P. Hughes and I. Aprahamian, *Nat. Chem.*, 2012, **4**, 757–762.
10 M. Stein, S. J. Middendorp, V. Carta, E. Pejo, D. E. Raines, S. A. Forman, E. Sigel and D. Trauner, *Angew. Chem., Int. Ed.*, 2012, **51**, 10500–10504.
11 S. Samanta, A. A. Beharry, O. Sadovski, T. M. McCormick, A. Babalhavaeji, V. Tropepe and G. A. Woolley, *J. Am. Chem. Soc.*, 2013, **135**, 9777–9784.
12 *Molecular Switches*, ed. B. L. Feringa, Wiley-VCH Verlag GmbH, 2001.
13 M.-M. Russew and S. Hecht, *Adv. Mater.*, 2010, **22**, 3348–3360.
14 J. García-Amorós and D. Velasco, *Beilstein J. Org. Chem.*, 2012, **8**, 1003–1017.
15 T. Fukaminato, T. Doi, N. Tamaoki, K. Okuno, Y. Ishibashi, H. Miyasaka and M. Irie, *J. Am. Chem. Soc.*, 2011, **133**, 4984–4990.
16 M. Berberich and F. Würthner, *Chem. Sci.*, 2012, **3**, 2771–2777.
17 M. Herder, M. Utecht, N. Manicke, L. Grubert, M. Pätzel, P. Saalfrank and S. Hecht, *Chem. Sci.*, 2013, **4**, 1028–1040.
18 A. Koçer, M. Walko, W. Meijberg and B. L. Feringa, *Science*, 2005, **309**, 755–758.
19 D. A. Davis, A. Hamilton, J. Yang, L. D. Cremar, D. Van Gough, S. L. Potisek, M. T. Ong, P. V. Braun, T. J. Martínez, S. R. White, J. S. Moore and N. R. Sottos, *Nature*, 2009, **459**, 68–72.
20 N. Tamaoki, K. Koseki and T. Yamaoka, *Angew. Chem., Int. Ed. Engl.*, 1990, **29**, 105–106.
21 J. M. Mativetsky, G. Pace, M. Elbing, M. A. Rampi, M. Mayor and P. Samorì, *J. Am. Chem. Soc.*, 2008, **130**, 9192–9193.
22 R. Reuter, N. Hostettler, M. Neuburger and H. A. Wegner, *Eur. J. Org. Chem.*, 2009, 5647–5652.
23 G. Haberhauer and C. Kallweit, *Angew. Chem., Int. Ed.*, 2010, **49**, 2418–2421.
24 P. K. Hashim and N. Tamaoki, *Angew. Chem., Int. Ed.*, 2011, **50**, 11729–11730.

25 S. Bellotto, R. Reuter, C. Heinis and H. A. Wegner, *J. Org. Chem.*, 2011, **76**, 9826–9834.
26 R. Reuter and H. A. Wegner, *Org. Lett.*, 2011, **13**, 5908–5911.
27 W. Szymański, B. Wu, C. Poloni, D. B. Janssen and B. L. Feringa, *Angew. Chem., Int. Ed.*, 2013, **52**, 2068–2072.
28 R. Reuter and H. A. Wegner, *Beilstein J. Org. Chem.*, 2012, **8**, 877–883.
29 Z. Yu, S. Weidner, T. Risse and S. Hecht, *Chem. Sci.*, 2013, **4**, 4156–4167.
30 H. Rau, *Angew. Chem., Int. Ed. Engl.*, 1973, **12**, 224–235.
31 J. Griffiths, *Chem. Soc. Rev.*, 1972, **1**, 481–493.
32 R. Siewertsen, H. Neumann, B. Buchheim-Stehn, R. Herges, C. Näther, F. Renth and F. Temps, *J. Am. Chem. Soc.*, 2009, **131**, 15594–15595.
33 D. Bléger, J. Schwarz, A. M. Brouwer and S. Hecht, *J. Am. Chem. Soc.*, 2012, **134**, 20597–20600.
34 Y. Yang, R. P. Hughes and I. Aprahamian, *J. Am. Chem. Soc.*, 2012, **134**, 15221–15224.
35 A. A. Beharry, O. Sadovski and G. A. Woolley, *J. Am. Chem. Soc.*, 2011, **133**, 19684–19687.
36 H. Rau and E. Lueddecke, *J. Am. Chem. Soc.*, 1982, **104**, 1616–1620.
37 H. Rau and S. Yu-Quan, *J. Photochem. Photobiol., C*, 1988, **42**, 321–327.
38 L. Wang, J. Xu, H. Zhou, C. Yi and W. Xu, *J. Photochem. Photobiol., C*, 2009, **205**, 104–108.
39 J. Garcia-Amorós, A. Sánchez-Ferrer, W. A. Massad, S. Nonell and D. Velasco, *Phys. Chem. Chem. Phys.*, 2010, **12**, 13238.
40 H. M. D. Bandara and S. C. Burdette, *Chem. Soc. Rev.*, 2012, **41**, 1809–1825.
41 R. Reuter and H. A. Wegner, *Chem. Commun.*, 2011, **47**, 12267–12276.
42 C. Grave and A. D. Schlüter, *Eur. J. Org. Chem.*, 2002, 3075–3098.
43 P. Kissel, J. van Heijst, R. Enning, A. Stemmer, A. D. Schlüter and J. Sakamoto, *Org. Lett.*, 2010, **12**, 2778–2781.
44 G. Ohlendorf, C. W. Mahler, S.-S. Jester, G. Schnakenburg, S. Grimme and S. Höger, *Angew. Chem., Int. Ed.*, 2013, **52**, 12086–12090.
45 T. Naddo, Y. Che, W. Zhang, K. Balakrishnan, X. Yang, M. Yen, J. Zhao, J. S. Moore and L. Zang, *J. Am. Chem. Soc.*, 2007, **129**, 6978–6979.
46 M. Fritzsche, A. Bohle, D. Dudenko, U. Baumeister, D. Sebastiani, G. Richardt, H. W. Spiess, M. R. Hansen and S. Höger, *Angew. Chem., Int. Ed.*, 2011, **50**, 3030–3033.
47 N. Tamaoki, K. Ogata, K. Koseki and T. Yamaoka, *Tetrahedron*, 1990, **46**, 5931–5942.
48 N. Tamaoki and T. Yamaoka, *J. Chem. Soc., Perkin Trans. 2*, 1991, 873–878.
49 Y. Norikane, K. Kitamoto and N. Tamaoki, *J. Org. Chem.*, 2003, **68**, 8291–8304.
50 For a double porphyrin bridged by four azobenzene units see: K. H. Neumann and F. Vögtle, *J. Chem. Soc., Chem. Commun.*, 1988, 520–522.
51 D. Gräf, H. Nitsch, D. Ufermann, G. Sawitzki, H. Patzelt and H. Rau, *Angew. Chem., Int. Ed. Engl.*, 1982, **21**, 373–374.
52 N. Tamaoki, K. Koseki and T. Yamaoka, *Tetrahedron Lett.*, 1990, **31**, 3309–3312.
53 Y. Norikane, K. Kitamoto and N. Tamaoki, *Org. Lett.*, 2002, **4**, 3907–3910.
54 Y. Norikane and N. Tamaoki, *Eur. J. Org. Chem.*, 2006, 1296–1302.
55 M. Müri, K. C. Schuermann, L. De Cola and M. Mayor, *Eur. J. Org. Chem.*, 2009, 2562–2575.
56 R. Reuter and H. A. Wegner, *Chem.–Eur. J.*, 2011, **17**, 2987–2995.
57 J. Robertus, S. F. Reker, T. C. Pijper, A. Deuzeman, W. R. Browne and B. L. Feringa, *Phys. Chem. Chem. Phys.*, 2012, **14**, 4374–4382.
58 D. Bléger, J. Dokić, M. V. Peters, L. Grubert, P. Saalfrank and S. Hecht, *J. Phys. Chem. B*, 2011, **115**, 9930–9940.
59 L. Schweighauser and H. A. Wegner, *Chem. Commun.*, 2013, **49**, 4397–4399.
60 P. Müller, I. Usón, V. Hensel, A. D. Schlüter and G. M. Sheldrick, *Helv. Chim. Acta*, 2001, **84**, 778–785.
61 A. D. Finke, D. E. Gross, A. Han and J. S. Moore, *J. Am. Chem. Soc.*, 2011, **133**, 14063–14070.
62 The line broadening and loss in fine structure of the 10 mg ml^{-1} spectrum are caused by the imperfect shimming due to the changes in concentration.
63 Y. Norikane, Y. Hirai and M. Yoshida, *Chem. Commun.*, 2011, **47**, 1770–1772.
64 R. Reuter and H. A. Wegner, *Chem. Commun.*, 2012, **49**, 146–148.
65 For an example with *in situ* laser irradiation see: K. M. Tait, J. A. Parkinson, S. P. Bates, W. J. Ebenezer and A. C. Jones, *J. Photochem. Photobiol., C*, 2003, **154**, 179–188.
66 H. Kuhn, *J. Chem. Phys.*, 1949, **17**, 1198–1212.
67 The Gaussian 09 software package was utilized to optimize the structures and calculate the frequencies: M. J. Frisch, *et al.*, *Gaussian 09 (Revision D.01 and A.02)*, Gaussian Inc., Wallingford CT, 2009.
68 E. Fanghänel, K. Behrmann, E. Bauwe, J. B. Kyziol and W. Waslawek, *Z. Für Chem.*, 1984, **24**, 286–287.